SUPPLEMENTAL MATERIAL

Langlais et al., http://www.jem.org/cgi/content/full/jem.20151764/DC1

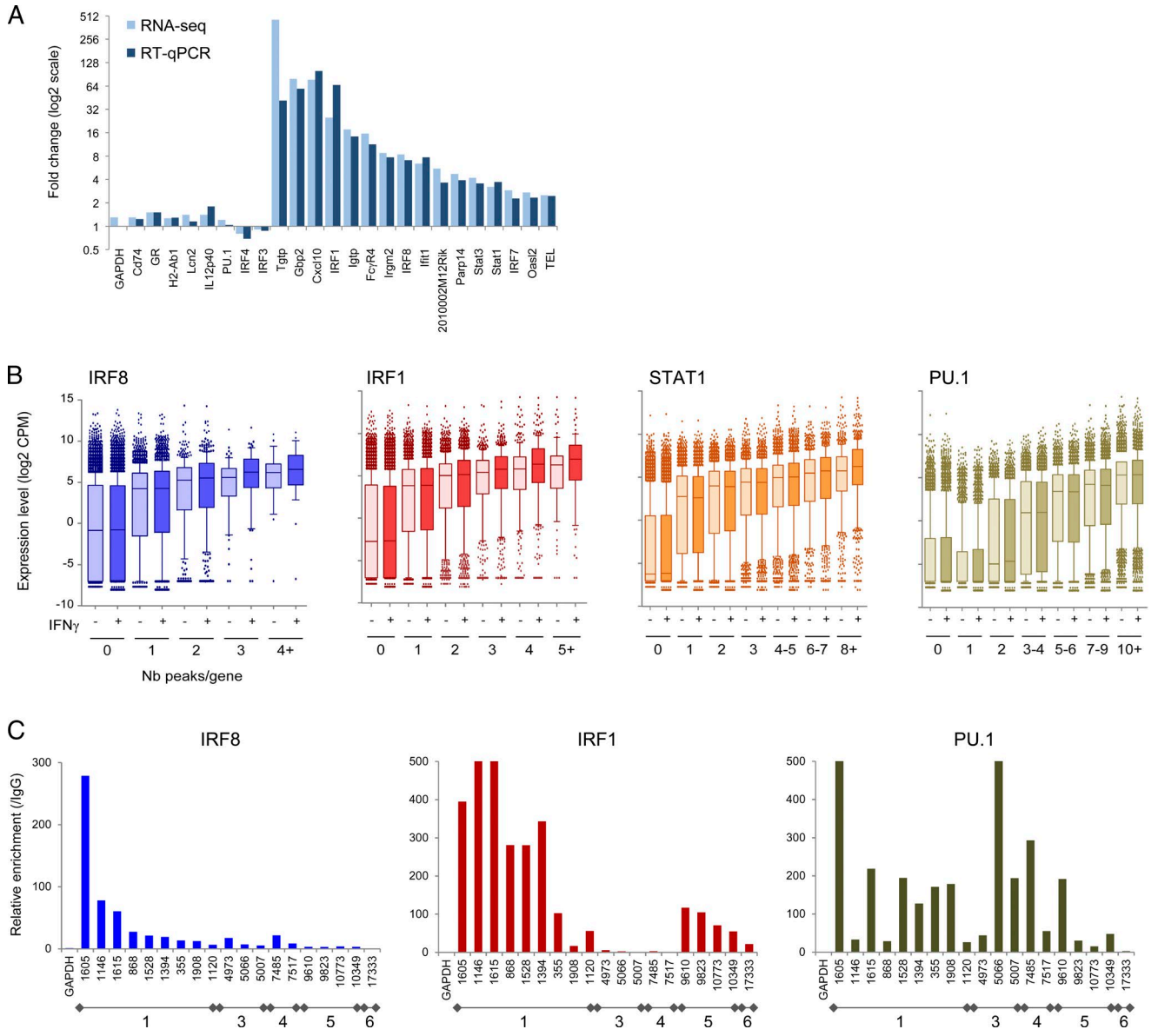

Figure S1. **Validation of RNA seq and ChIP seq data and association of gene expression with presence of TF binding sites.** (A) The macrophage transcriptional response to IFN-γ identified by RNA seq was validated by qPCR using B6 BMDMs treated or not treated with IFN-γ for 3 h and for genes responsive (n = 16) and nonresponsive to IFN-γ (n = 8). The qPCR results confirmed the nonresponsiveness of eight genes and the IFN-γ activation of 16 genes. qPCR gene expression results were normalized to *Gapdh* used as an internal control. A representative set of at least three independent experiment is shown. (B) Box plots presenting the normalized gene expression level (log2 counts per million reads; log2[CPM]) before and after IFN-γ treatment; genes are grouped by the number of TF binding peaks within 20 kb of their transcription start site. (C) The ChIP seq generated in this study was validated using independent ChIP on B6 BMDMs treated with IFN-γ for 3 h. The relative enrichment was calculated over control IgG and normalized by *Gapdh* negative control region. ChIP seq binding peaks from clusters 1, 3, 4, 5, and 6 were validated. The expected binding patterns were validated with recruitment of IRF8 on clusters 1, 3, and 4, IRF1 on clusters 1, 5, and 6, and PU.1 on clusters 1, 3, 4, and 5. A representative of at least two independent experiment is shown.

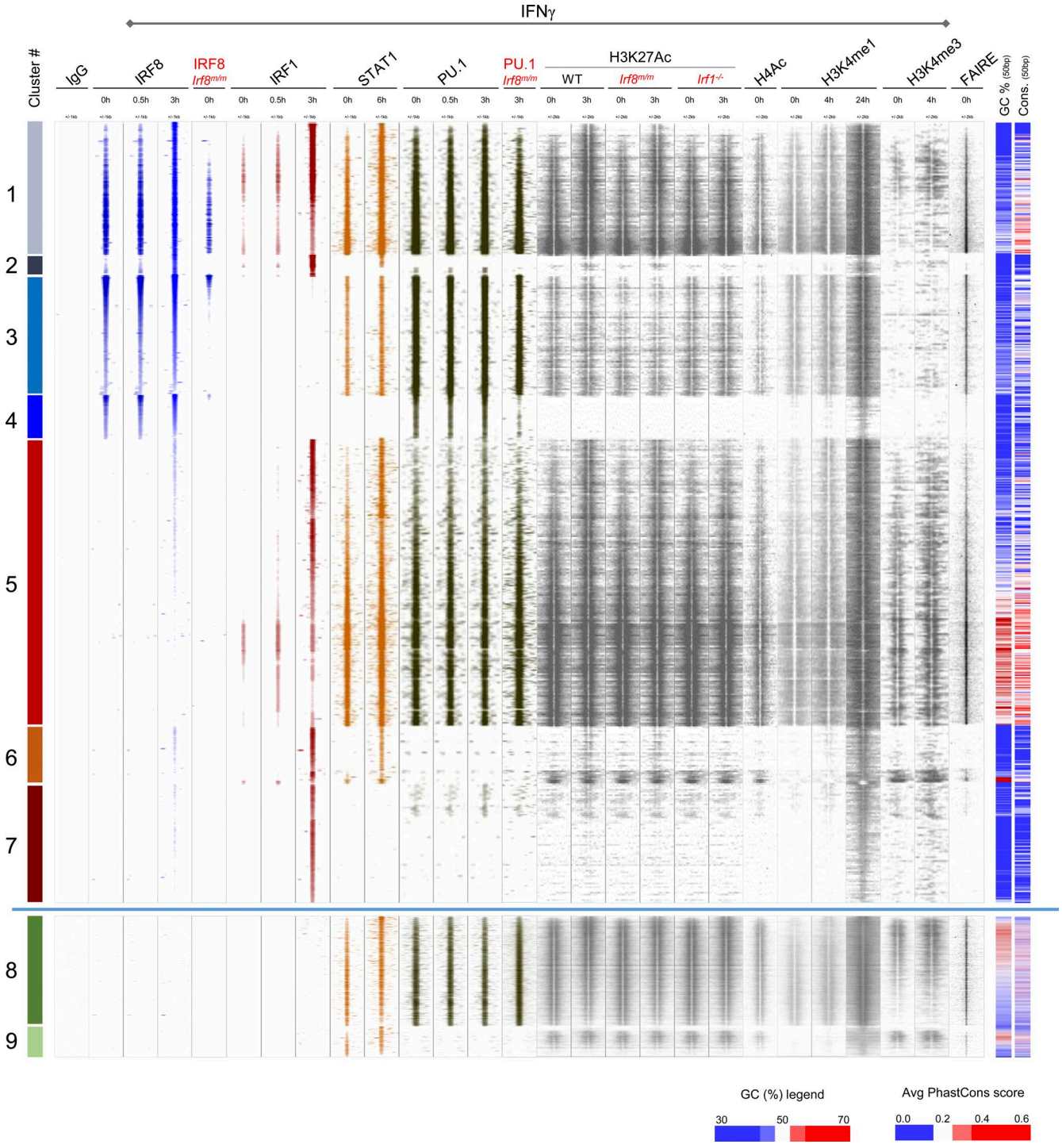

Figure S2. **Heatmap showing genomic binding profiles of selected TFs and epigenetic characteristics of the corresponding binding clusters.** Heatmap defining the nine TF binding schemes in Fig. 2 B. Each horizontal line presents the ChIP sequence read density in a ±1-kb region around a unique position and ±2 kb for epigenetic datasets. ChIP seq for H4Ac (Chen et al., 2012), H3K4me1, and H3K4me3 histone modifications and FAIRE chromatin accessibility dataset (Ostuni et al., 2013) were reanalyzed as described in Materals and methods, and read density profiles were extracted for ±2 kb around cluster binding peaks. Complete H3K27Ac epigenetic modification profiles are shown for ChIP seq in WT, *Irf8*$^{m/m}$, and *Irf1*$^{-/-}$ mutant BMDMs before and after 3 h of IFN-γ treatment. Finally, the guanine–cytosine content and mammalian genomic sequence conservation is shown for 50 bp surrounding each cluster binding peak.

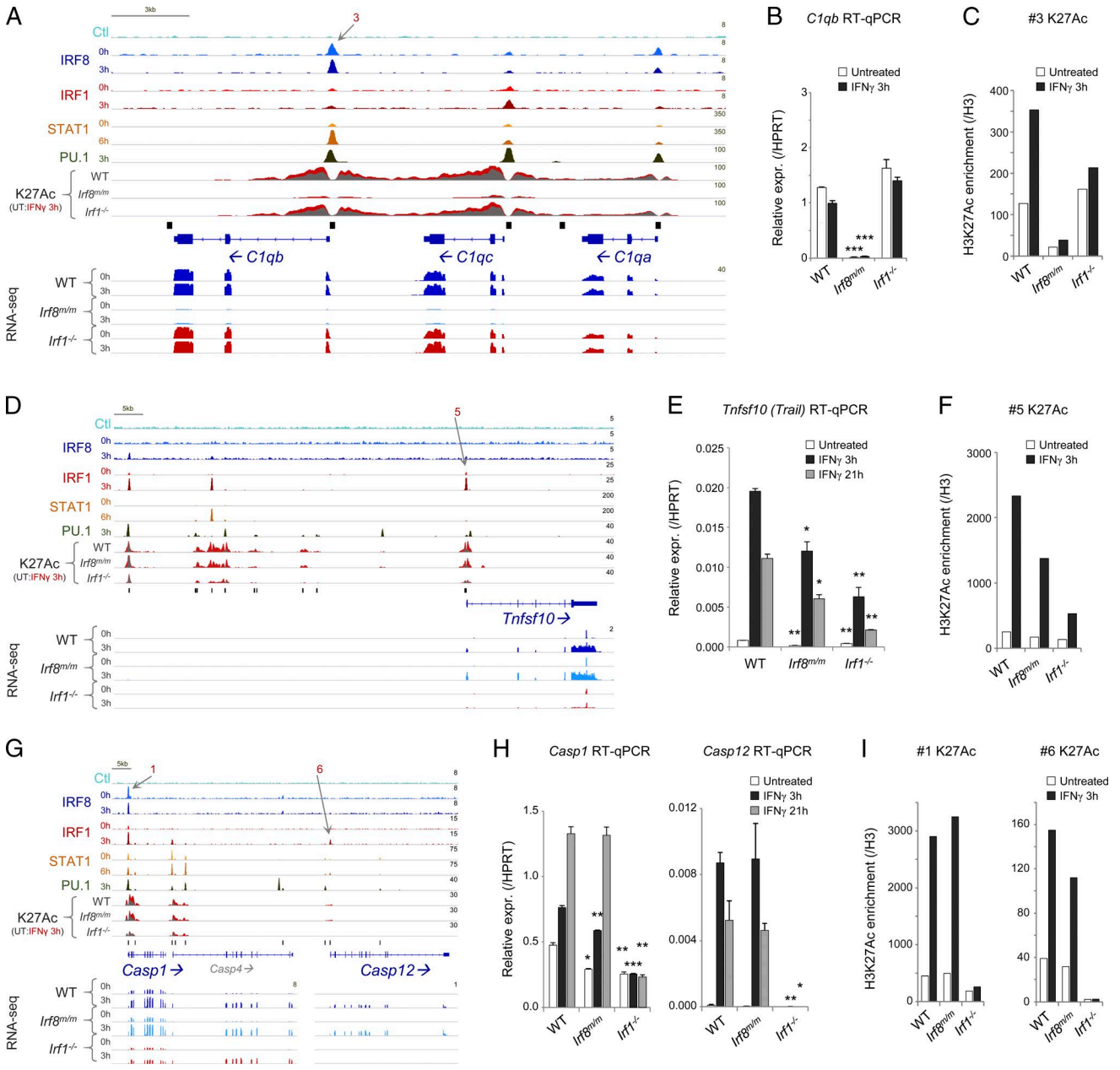

Figure S3. **Examples of IRF8-dependent basal regulation and of IRF1-dependent IFN-γ–induced transcription in BMDMs.** (A) Genomic snapshot of *C1q* locus as a representative example of IRF8-dependent regulation of basal gene expression in macrophages; density of ChIP seq reads (IRF8, IRF1, STAT1, PU.1, and H3K27Ac) and RNA seq reads (WT, IRF8, and IRF1 mutants) are shown. (B) RT-qPCR validation of *C1qb* expression in WT and *Irf8*$^{m/m}$ and *Irf1*$^{-/-}$ mutant BMDMs (mean ± SD; p-values were calculated using Student's *t* test from independent biological replicates). (C) ChIP-qPCR validation of H3K27Ac levels (relative to histone H3) at the cluster 3 peak found at the *C1qb* promoter in WT and *Irf8*$^{m/m}$ and *Irf*$^{-/-}$ mutant BMDMs (data are representative of three independent experiments). (D–F) The *Tnfsf10* gene encodes TRAIL, a protein of the Tnf super family. The *Tnfsf10* locus harbors three cluster 5 peaks that acquire K27Ac mark after IFN-γ treatment, which is strongly impaired in *Irf1*$^{-/-}$ macrophages and as determined by ChIP-qPCR (the peak identified by an arrow was analyzed). (G–I) *Casp1* and *Casp12* inflammatory caspases are other examples of genes in which IFN-γ–driven transcriptional activation is severely impaired in *Irf1* mutant macrophages. *Tnfsf10* and *Casp1/12* genomic snapshot expression validation by qPCR and H3K27Ac ChIP are presented as in A–C; p-values were calculated using Student's *t* test. *, P ≤ 0.05; **, P ≤ 0.01; ***, P ≤ 0.001.

Table S1 is available as an Excel file and lists the genomic positions for the selected TF binding clusters. The list of TF binding sites is in the order presented in the Fig. 2 B heatmap; their binding scheme affiliation is indicated, as well as their genomic position and the position of the closest annotated gene.

Table S2 is available as an Excel file and lists the genes that showed altered expression at steady state in *Irf8*$^{m/m}$ and *Irf1*$^{-/-}$ mutant macrophages.

Table S3 is available as an Excel file and lists the genes regulated in response to IFN-γ treatment in *Irf8*$^{m/m}$ and *Irf1*$^{-/-}$ mutant macrophages.

Table S4 is available as an Excel file and lists the genes mutated in human PIDs and the forming part of the IRF8/IRF1 regulome.

Table S5 is available as an Excel file and lists oligonucleotide primers used for ChIP-qPCR and RT-qPCR in this study.

REFERENCES

Chen, X., I. Barozzi, A. Termanini, E. Prosperini, A. Recchiuti, J. Dalli, F. Mietton, G. Matteoli, S. Hiebert, and G. Natoli. 2012. Requirement for the histone deacetylase Hdac3 for the inflammatory gene expression program in macrophages. *Proc. Natl. Acad. Sci. USA.* 109:E2865–E2874. http://dx.doi.org/10.1073/pnas.1121131109

Ostuni, R., V. Piccolo, I. Barozzi, S. Polletti, A. Termanini, S. Bonifacio, A. Curina, E. Prosperini, S. Ghisletti, and G. Natoli. 2013. Latent enhancers activated by stimulation in differentiated cells. *Cell.* 152:157–171. http://dx.doi.org/10.1016/j.cell.2012.12.018